https://doi.org/10.1093/plphys/kiac144 PLANT PHYSIOLOGY 2022: 00: 1–5

Plant Physiology®

Letters

The impact of drought-induced root and root hair shrinkage on root–soil contact

Patrick Duddek ,[1,2] Andrea Carminati ,[1] Nicolai Koebernick ,[3] Luise Ohmann ,[4] Goran Lovric ,[5] Sylvain Delzon ,[6] Celia M. Rodriguez-Dominguez,[7] Andrew King [8] and Mutez Ali Ahmed[2,9,*,†]

1 Physics of Soils and Terrestrial Ecosystems, Department of Environmental Systems Science, Institute of Terrestrial Ecosystems, ETH Zürich, Universitätsstrasse 16, 8092 Zurich, Switzerland
2 Chair of Soil Physics, Bayreuth Center of Ecology and Environmental Research (BayCEER), University of Bayreuth, Universitätstrasse 30, 95447 Bayreuth, Germany
3 Soil Science and Soil Protection, Martin Luther University Halle-Wittenberg, Von-Seckendorff-Platz 3, 06120 Halle (Saale), Germany
4 Department of Soil System Science, Helmholtz Centre for Environmental Research, Theodor-Lieser-Str. 4, 06120 Halle (Saale), Germany
5 Swiss Light Source, Paul Scherrer Institute, Forschungsstrasse 111, 5232 Villigen, Switzerland
6 BIOGECO, INRA, Univ. Bordeaux, Allée Geoffroy St-Hilaire, 33615 Pessac, France
7 Irrigation and Crop Ecophysiology Group, IRNAS-CSIC, Avda. Reina Mercedes, 10, 41012 Sevilla, Spain
8 Synchrotron SOLEIL, L'Orme des Merisiers, 91192 Gif-sur-Yvette Cedex, France
9 Department of Land, Air and Water Resources, College of Agricultural and Environmental Sciences, University of California Davis, One Shields Avenue, Davis, CA 95616, United States

*Author for correspondence: maaahmed@ucdavis.edu
†Senior author.

M.A.A., A.C., and P.D. conceived and designed the experiments. M.A.A., N.K., and L.O. performed the experiments at TOMCAT. P.D., M.A.A., C.M.R.-D., and S.D. performed the experiments at SOLEIL. P.D. analyzed the data and wrote the manuscript with contributions from A.C., G.L., and M.A.A. G.L. and A.K. provided technical assistance as beamline scientists at TOMCAT (PSI, Switzerland) and SOLEIL (France). All authors contributed to editing and revising the manuscript.
The author responsible for distribution of materials integral to the findings presented in this article in accordance with the policy described in the Instructions for Authors (https://academic.oup.com/plphys/pages/General-Instructions) is: Mutez Ali Ahmed (maaahmed@ucdavis.edu).

Dear Editor,

Root hairs improve plant access to soil resources, especially under edaphic stress (Singh Gahoonia and Nielsen, 2004; Marin et al., 2020; Wissuwa and Kant, 2021). While root shrinkage and the formation of cortical lacunae limit the continuity of the liquid phase at the root–soil interface (Nobel and Cui, 1992; Carminati et al., 2009; Cuneo et al., 2016), the impact of edaphic stress on root hairs remains largely unknown. Here, we provide insights into drought-induced root and root hair shrinkage and the ramification on root–soil contact. We used high-resolution synchrotron radiation X-ray micro-CT (actual pixel size: 0.65 × 0.65 μm^2) to visualize roots, root hairs, and root–soil contact of maize (*Zea mays* L.). The mean root hair length and diameter were 245.5 ± 50.2 µm and 17.88 ± 0.99 µm, respectively. Although root hairs substantially increased root–soil contact, we found that, during soil drying, their shrinkage was initiated at relatively high soil matric potentials (between −10 and −310 kPa). Root hair shrinkage represents the first step within a sequence of root responses to progressive soil drying, followed by the initiation of cortical lacunae and root shrinkage. The latter leads to air filled gaps at the root–soil interface. All these processes coincide with a gradual disconnection of roots from soil and hence a severe reduction of root–soil contact during soil drying.

We grew maize in 3D printed microcosms (Keyes et al., 2013) filled with a loamy substrate. Plants were placed in a climate chamber at a relative humidity of 65% and a

Received November 29, 2021. Accepted March 05, 2022. Advance access publication March 24, 2022
© American Society of Plant Biologists 2022. All rights reserved. For permissions, please email: journals.permissions@oup.com

Downloaded from https://academic.oup.com/plphys/advance-article/doi/10.1093/plphys/kiac144/6553680 by INRA AVIGNON user on 11 May 2022

temperature of 22°C during day and 18°C at night. Synchrotron radiation X-ray micro-CT was performed at the X02DA TOMCAT beamline of Swiss Light Source (SLS) and the PSICHE beamline of Synchrotron SOLEIL (Saclay, France). Image processing was conducted in Avizo (Thermo Fisher Scientific, 2019). The experimental setup and image processing is detailed in the Supplemental Methods.

Eight independent plants comprising 16 samples were analyzed. We observed that not only roots, but also root hairs lost turgidity during soil drying (Figure 1). Shrunk hairs appeared as 2D surfaces forming twisted and folded fibrous structures (Supplemental Figure S1). Figure 1 illustrates a turgid root with turgid hairs (Figure 1A), a turgid root with shrunk hairs (Figure 1B), as well as a shrunk root, with shrunk hairs, showing severe cortex drying (Figure 1C). Figure 1D depicts a 3D rendered sample containing turgid root hairs, while Figure 1E shows a region near the root tip containing only shrunk hairs behind the elongation zone. A 2D slice of the latter illustrates hair shrinkage more clearly (Figure 1F).

We grouped the samples according to root hair shrinkage and cortex drying as follows (Supplemental Figure S2):

- Group 1: $> 50\%$ hair shrinkage.
- Group 2: $> 90\%$ hair shrinkage $\wedge > 10\%$ cortex drying.
- Group 3: $> 50\%$ cortex drying.

We estimated the local volumetric soil water content (θ_v) of each sample from the grayscale values of the micropore region, which depend on the volumetric fraction of water and solid grains within this region. Our approach is justified because macropores were drained and water was only retained in the micropore region (see Supplemental Methods for details). Besides, we measured the soil matric potential using a WP4C dewpoint psychrometer (Decagon Devices, Pullman, Washington, USA) and the gravimetric soil water content (θ_g) of four additional samples. Since the WP4C is only accurate below a potential of approximately −100 kPa, we further estimated the soil matric potential of the wettest sample based on the θ_g, the bulk density, and the water retention curve (Vetterlein et al., 2021; Figure 2A).

At this spatial scale, estimating soil water status is challenging and prone to errors, and the relation between water potential and water content is very heterogeneous. The measured gravimetric soil water content and soil matric potential might not be representative of the imaged region (which is only a small fraction of the soil sample). The estimated image-based water content (volume of water relative to the whole soil domain) relies on the assumption of constant macro- and microporosity across the samples. While this might be valid for the microporosity, it is not for the macroporosity. Yet, since the macropores were drained, our approach to estimate the soil water content is legit. A comparison of volumetric soil water content based on grayscale and gravimetric measurements (Supplemental Figure S4) as well as a discussion on additional sources of uncertainty is available in the Supplemental Methods.

As root and root hair shrinkage depend on soil matric potential, we interpret our results primarily in the framework of matric potential measured by WP4C. We found that hairs were fully turgid up to a matric potential of −10 kPa, ($\theta_v \approx 0.27 \frac{mm^3}{mm^3}$; Figure 2A). A substantial fraction of hairs (up to 70%) shrank at potentials ranging from −10 to −310 kPa ($\theta_v \approx 0.25 \frac{mm^3}{mm^3}$). At matric potentials between −310 and −970 kPa ($\theta_v \approx 0.19 \frac{mm^3}{mm^3}$), we observed a hair shrinkage of 40% to 100%. Except for two samples at $\theta_v \approx 0.16 \frac{mm^3}{mm^3}$ (approximately 70% hair shrinkage), no turgid hairs were visible below this potential. Figure 2A illustrates a positive association between soil drying and root/root hair shrinkage as well as cortex drying. Compared with hair shrinkage, the onset of both cortex drying and root shrinkage occurred more gradually and at a more negative soil matric potential (below −1,000 kPa).

The percentage of root hair surface area in contact to soil was significantly ($p = 0.029$) higher (0.40 ± 0.03) compared with the epidermis surface area (0.16 ± 0.04) (Figure 2B). We compared the macro porosity ϕ (measured within a hollow cylinder with inner surface corresponding to the root–soil interface and thickness of d = 10 μm) to the fraction of root–soil contact, defined as the contact surface $A_{Contact}$ normalized over the epidermis surface area $A_{Epidermis}$ (Figure 2C). Note that $\frac{A_{Contact}}{A_{Epidermis}} = \lim_{d \to 0} 1 - \phi$. The contact surface of the majority of samples within groups 2 and 3 was considerably below the expected value of $1-\phi$ (shown as a solid line in Figure 2C). The contact exceeded the expected value when root and a fraction of hairs were turgid (group 1). Additionally, even for decreasing porosities, we observed a decreasing normalized contact (Figure 2C). This is caused by the decreasing turgidity of the root cortex and the accompanying root shrinkage (Figure 2D). As soil dried, root cortex shrank and roots lost contact to the soil matrix.

In summary, our data show a drought-induced disconnection of roots from soil starting from the hairs. Although root hairs are believed to play a key role in water and nutrient uptake, their shrinkage severely reduces the root–soil contact in the rhizosphere. This may increase the interfacial resistance between roots and soil and limit uptake processes. Indeed, a recent study on the impact of hairs on water uptake showed that, in maize, hairs had a minor, if any, contribution to soil–plant hydraulics (Cai et al., 2021). This might be caused by hair shrinkage and/or by the relatively short length of maize root hairs (0.2–0.4mm) (Cai et al., 2021). In barley, which has longer hairs (0.6–0.8 mm, (Burak et al., 2021)), root hairs facilitated water uptake under dry soil conditions, both in the laboratory and under field conditions (Carminati et al., 2017; Marin et al., 2020).

Root hair shrinkage does not only depend on soil matric potential, but also on age. Root hair life span ranges from 2 d (Fusseder, 1987; Jungk, 2001) up to 21 d (Xiao et al., 2020). The observation of entire hair shrinkage just behind the root elongation zone (Figure 1E) proves that hair shrinkage is not solely caused by aging. Interestingly, hair shrinkage

Downloaded from https://academic.oup.com/plphys/advance-article/doi/10.1093/plphys/kiac144/6553680 by INRA AVIGNON user on 11 May 2022

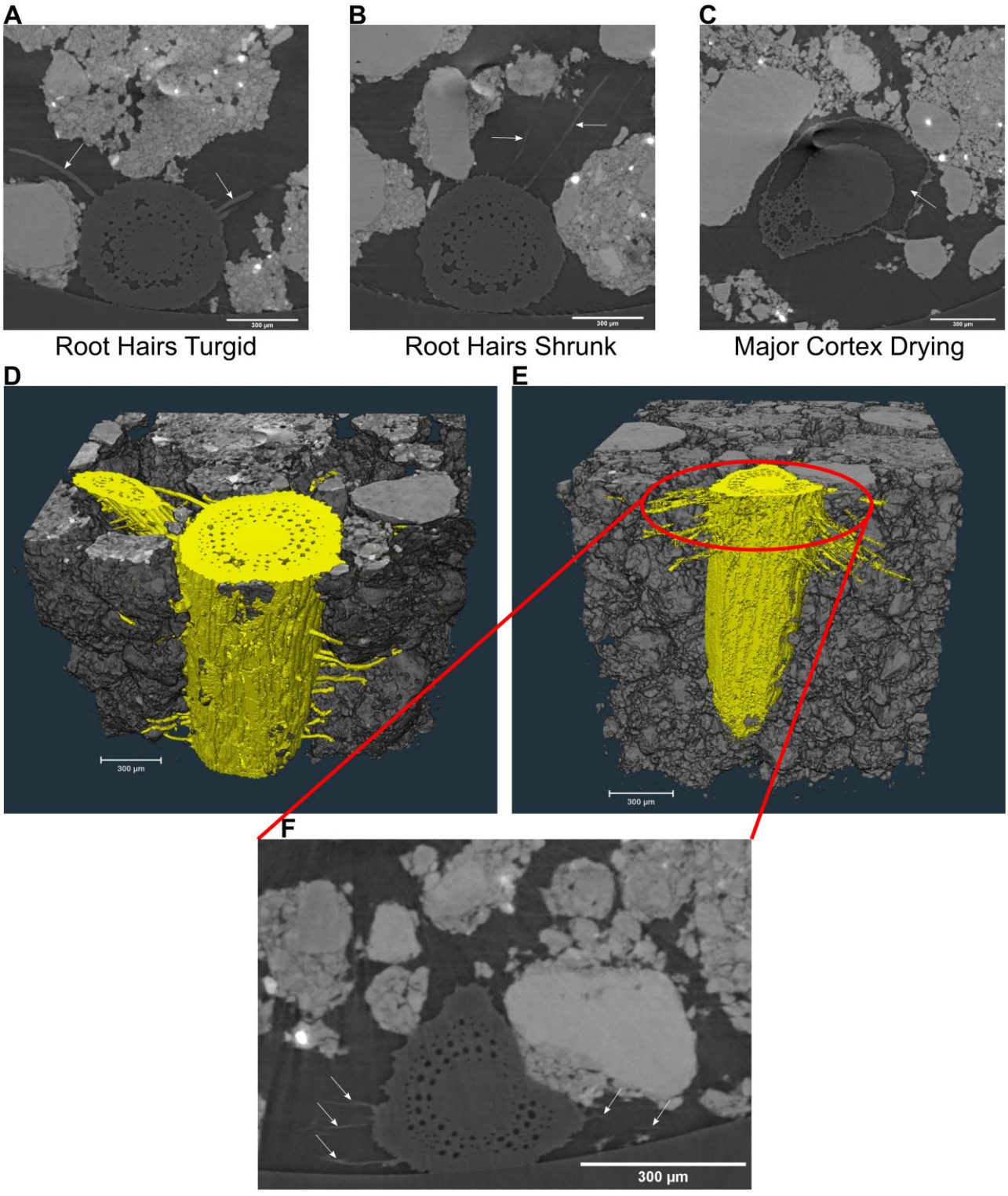


Figure 1 Collection of reconstructed 2D slices and 3D renderings illustrating different root stages. A, Both root and root hairs are turgid (arrows pointing at turgid root hairs, scale bar = 300 µm). B, While the main root is turgid, hairs have shrunk (arrows pointing at shrunk root hairs, scale bar = 300 µm). C, Severe cortex drying (arrow pointing at the air-filled space between epidermis and endodermis, scale bar = 300 µm). D, 3D rendering of a seminal root compartment containing a lateral root and turgid root hairs surrounded by soil matrix (scale bar = 300 µm). E, 3D rendering of a root compartment near the root tip showing shrunk root hairs behind the elongation zone (scale bar = 300 µm). F, 2D slice near the root tip (arrows pointing at shrunk root hairs, scale bar = 300 µm).

Downloaded from https://academic.oup.com/plphys/advance-article/doi/10.1093/plphys/kiac144/6553680 by INRA AVIGNON user on 11 May 2022

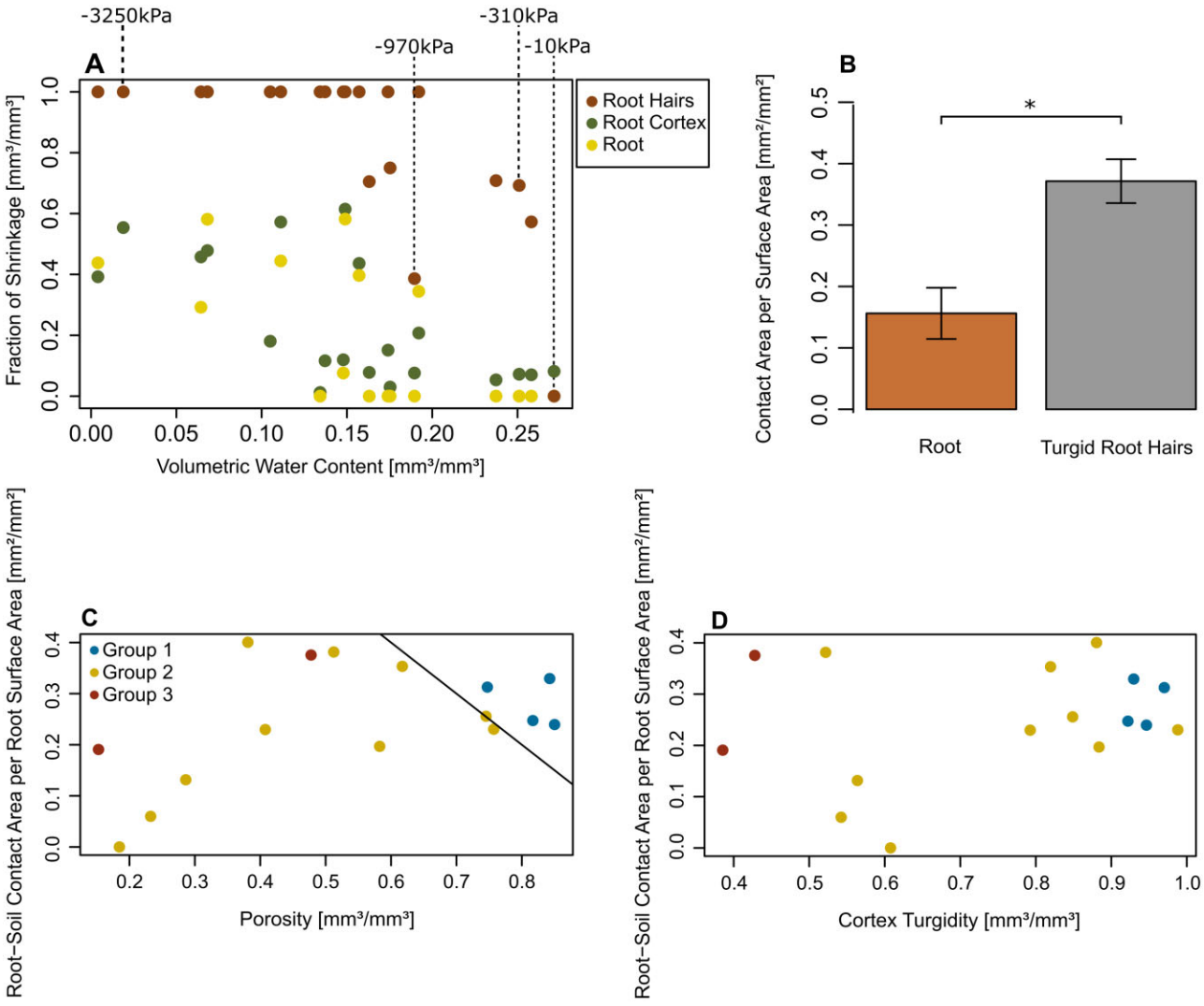


Figure 2 Quantification of root/root hair shrinkage and root–soil contact. A, Association between the volumetric soil water content and root shrinkage, root hair shrinkage, and root cortex drying (note that root hair shrinkage was not quantified based on hair volume but on the number of hairs). The onset of root shrinkage and cortex drying was at later stages of soil drying (below −1,000 kPa) and occurred more gradually than root hair shrinkage. The values assigned to four samples represent the soil matric potential calculated based on the gravimetric soil water content, bulk density, and water retention curve (−10 kPa) and the measured matric potential using WP4C (rest). B, Soil contact area of turgid root and root hairs normalized by the corresponding surface area. The bar chart highlights a significant difference ($p = 0.029$ (Mann–Whitney U test)) between roots and root hairs (error bars indicate standard deviation). C, The expected root–soil contact fraction based on the macroporosity at the root–soil interface (indicated by the solid line $f(\phi) = 1 - \phi$) was not met by the majority of the samples. However, roots having turgid hairs exceeded the expectation value. D, Cortex turgidity and accompanying root shrinkage explains the deviation of the normalized contact from the expectation values in (C).

was root type dependent. The presence of turgid hairs on the laterals in the immediate vicinity of severely shrunk seminal roots (Supplemental Figure S3) is intriguing and requires further investigation.

Supplemental data

The following materials are available in the online version of this article.

Supplemental Figure S1. Comparison of turgid and shrunk root hairs in 2D and 3D.

Supplemental Figure S2. Data clustering.

Supplemental Figure S3. Root hairs of different root types.

Supplemental Figure S4. Volumetric soil water content.

Supplemental Methods.

Acknowledgments

This project was carried out in the framework of the priority program 2089 "Rhizosphere spatiotemporal organization — a key to rhizosphere functions" funded by DFG, German Research Foundation (project number 403670197). We thank Caroline Marcon and Frank Hochholdinger (University of Bonn) for providing the maize B73 seeds. We also thank

Downloaded from https://academic.oup.com/plphys/advance-article/doi/10.1093/plphys/kiac144/6553680 by INRA AVIGNON user on 11 May 2022

Patrick von Jeetze (Potsdam Institute for Climate Impact) for assistance with sample preparation and data collection. The authors acknowledge the Paul Scherrer Institute, Villigen, Switzerland as well as the Synchrotron SOLEIL, Saclay, France, for provision of synchrotron radiation beamtime at beamline X02DA TOMCAT of the SLS and PSICHE beamline of Synchrotron SOLEIL.

Funding

The authors acknowledge the Deutsche Forschungsgemeinschaft (DFG, German Research Foundation) for funding of the priority program 2089, project number 403670197 "Emerging effects of root hairs and mucilage on plant scale soil water relations" to M.A.A. and A.C.

Conflict of interest statement. The authors declare no conflict of interest.

References

Burak E, Quinton JN, Dodd IC (2021) Root hairs are the most important root trait for rhizosheath formation of barley (*Hordeum vulgare* L.), maize (*Zea mays* L.), and *Lotus japonicus* (Gifu). Ann Bot doi:10.1093/aob/mcab029

Cai G, Carminati A, Abdalla M, Ahmed MA (2021) Soil textures rather than root hairs dominate water uptake and soil–plant hydraulics under drought. Plant Physiol doi:10.1093/plphys/kiab271

Carminati A, Passioura JB, Zarebanadkouki M, Ahmed MA, Ryan PR, Watt M, Delhaize E (2017) Root hairs enable high transpiration rates in drying soils. New Phytol **216**: 771–781

Carminati A, Vetterlein D, Weller U, Vogel H-J, Oswald SE (2009) When roots lose contact. Vadose Zone J **8**: 805–809

Cuneo IF, Knipfer T, Brodersen CR, McElrone AJ (2016) Mechanical failure of fine root cortical cells initiates plant hydraulic decline during drought. Plant Physiol **172**: 1669–1678

Fusseder A (1987) The longevity and activity of the primary root of maize. Plant Soil **101**: 257–265

Jungk A (2001) Root hairs and the acquisition of plant nutrients from soil. J Plant Nutr Soil Sci **164**: 121–129.

Keyes SD, Daly KR, Gostling NJ, Jones DL, Talboys P, Pinzer BR, Boardman R, Sinclair I, Marchant A, Roose T (2013) High resolution synchrotron imaging of wheat root hairs growing in soil and image based modelling of phosphate uptake. New Phytol **198**: 1023–1029

Marin M, Feeney DS, Brown LK, Naveed M, Riuz S, Koebernick N, Bengough AG, Hallett PD, Roose T, Puértolas J, et al. (2020) Significance of root hairs for plant performance under contrasting field conditions and water deficit. Ann Bot doi:10.1093/aob/mcaa181

Nobel PS, Cui M (1992) Hydraulic conductances of the soil, the root–soil air gap, and the root: changes for desert succulents in drying soil. J Exp Bot **43**: 319–326

Singh Gahoonia T, Nielsen NE (2004) Root traits as tools for creating phosphorus efficient crop varieties. Plant Soil **260**: 47–57

Thermo Fisher Scientific (2019) Avizo Software for Materials Research: Materials Characterization and Quality Control (Reprint). Available online: https://assets.thermofisher.com/TFS-Assets/MSD/brochures/brochure-avizo-software-materials-research.pdf

Vetterlein D, Lippold E, Schreiter S, Phalempin M, Fahrenkampf T, Hochholdinger F, Marcon C, Tarkka M, Oburger E, Ahmed M, et al. (2021) Experimental platforms for the investigation of spatiotemporal patterns in the rhizosphere-laboratory and field scale. J Plant Nutr Soil Sci doi:10.1002/jpln.202000079

Wissuwa M, Kant J (2021) Does half a millimetre matter? Root hairs for yield stability. A commentary on 'Significance of root hairs for plant performance under contrasting field conditions and water deficit'. Ann Bot doi:10.1093/aob/mcab027

Xiao S, Liu L, Zhang Y, Sun H, Zhang K, Bai Z, Dong H, Li C (2020) Fine root and root hair morphology of cotton under drought stress revealed with RhizoPot. J Agron Crop Sci **206**: 679–693

Downloaded from https://academic.oup.com/plphys/advance-article/doi/10.1093/plphys/kiac144/6553680 by INRA AVIGNON user on 11 May 2022